Current Research in Microbial Sciences 7 (2024) 100316

Contents lists available at ScienceDirect

Current Research in Microbial Sciences

journal homepage: www.sciencedirect.com/journal/current-research-in-microbial-sciences

Candida albicans enhances *Staphylococcus aureus* virulence by progressive generation of new phenotypes

Betsy Verónica Arévalo-Jaimes [a,b], Eduard Torrents [a,b,*]

[a] Bacterial infections and antimicrobial therapies group, Institute for Bioengineering of Catalonia (IBEC), Baldiri Reixac Street 10, 08037, Barcelona, Spain
[b] Microbiology Section, Department of Genetics, Microbiology and Statistics, Faculty of Biology, University of Barcelona, Diagonal Street 647, 08028, Barcelona, Spain

ARTICLE INFO

Keywords:
Galleria mellonella
Polymicrobial interactions
Interkingdom interactions
Synergistic effects
Proximity assay
Agr system
Pathogenicity

ABSTRACT

Candida albicans and *Staphylococcus aureus* have been co-isolated from several biofilm-associated diseases, including those related to medical devices. This association confers advantages to both microorganisms, resulting in detrimental effects on the host. To elucidate this phenomenon, the present study investigated colony changes derived from non-physical interactions between *C. albicans* and *S. aureus*. We performed proximity assays by confronting colonies of the yeast and the bacteria on agar plates at six different distances for 9-10 days. We found that colony variants of *S. aureus* originated progressively after prolonged exposure to *C. albicans* proximity, specifically in response to pH neutralization of the media by the fungi. The new phenotypes of *S. aureus* were more virulent in a *Galleria mellonella* larvae model compared to colonies grown without *C. albicans* influence. This event was associated with an upregulation of RNA III and a*grA* expression, suggesting a role for α-toxin. Our findings indicate that *C. albicans* enhances *S. aureus* virulence by inducing the formation of more aggressive colonies. This highlights the importance of understanding the intricate connection between environmental responses, virulence and, fitness in *S. aureus* pathogenesis.

1. Introduction

In the past, Koch's postulates helped identify the etiological causes of several monomicrobial infections (Todd and Peters, 2019c). Then, high-throughput genome sequencing techniques significantly expanded the notion of microbial biodiversity harboured within the body, revealing, for instance, more than 1000 species residing in the gut (Todd and Peters, 2019c). Currently, it is recognized that the coexistence of multiple microorganisms in the same host niche fosters interactions among them that can drive disease onset and outcome (Todd and Peters, 2019c). Furthermore, these complex communities can adopt the biofilm mode of life, secreting an extracellular matrix that surrounds and protects them from environmental attacks, including antimicrobial agents (Carolus, et al., 2019, Todd and Peters, 2019c).

Among the polymicrobial infections, those involving the presence of fungi and bacteria are particularly significant in the clinical context (Carolus, et al., 2019). The yeast *Candida albicans* and the Gram-positive bacterium *Staphylococcus aureus* are among the most prevalent nosocomial pathogens responsible for severe morbidity and mortality (Todd et al., 2019a). This duo is frequently present in intra-abdominal infections that can disseminate and produce systemic infections that are very difficult to treat (Carolus, et al., 2019, Todd and Peters, 2019c). Moreover, *C. albicans* and *S. aureus* have been co-isolated from several biofilm-associated diseases, including chronic wound infections, cystic fibrosis, urinary tract infections, and medical-device-related infections (Carolus, et al., 2019, Todd and Peters, 2019c). Being part of these polymicrobial biofilms confers several advantages to both members, such as enhanced tolerance to vancomycin in *S. aureus* (Kong, et al., 2016) and to miconazole in *C. albicans* (Kean, et al., 2017). Likewise, the addition of a conditioned medium from *S. aureus* dramatically increases *C. albicans* biofilm growth (Lin, et al., 2013).

These microorganisms' cooperative relationship involves physical interactions and interspecies communication (Carolus, et al., 2019, Eichelberger and Cassat, 2021). The chemical interactions between *C. albicans* and *S. aureus* include secreted molecules from the quorum sensing (QS) system (Carolus, et al., 2019, Todd and Peters, 2019c). In *S. aureus*, the best-characterized QS system is the accessory regulatory (*agr*) system, consisting of the promoter P2 and P3 that drive the expression of the transcripts RNA II and RNA III, respectively (Todd and Peters, 2019c). RNA II is encoded for four genes: *agrA, agrB, agrC* and *agrD*. AgrB is a membrane protein that modifies and secretes the pre-signal peptide AgrD into its mature form, the autoinducing peptide 2

* Corresponding author at: Institute for Bioengineering of Catalonia (IBEC), Baldiri Reixac Street 10, 08037, Barcelona, Spain
E-mail addresses: etorrents@ibecbarcelona.eu, eduard.torrents@ub.edu (E. Torrents).

https://doi.org/10.1016/j.crmicr.2024.100316

Available online 17 November 2024

(AIP-2). AIP-2 is recognized by the membrane-bound protein kinase AgrC, which phosphorylates AgrA, activating P2 and P3. RNA III is the effector molecule of the *agr* system and is responsible for toxin production, including α-toxin, a fundamental tool in *S. aureus*' pathogenicity (Todd and Peters, 2019c).

Polymicrobial infections are often associated with poor patient prognosis (Eichelberger and Cassat, 2021, Peters, et al., 2012). In the case of *C. albicans* and *S. aureus*, it has long been known that their intraperitoneal coinfection has a synergistic effect on mouse mortality (Carlson, 1982). Increased virulence of *C. albicans* and *S. aureus* coinfection has also been reported in zebrafish embryos, *Galleria mellonella* larvae, and patients with systemic infections (Sheehan, et al., 2020, Wu, et al., 2021). However, it was only recently that the major lethality driver and its activation mechanism were identified. *C. albicans* ribose catabolism and alkalinization of the extracellular pH led to sustained activation of the staphylococcal *agr* system (Saikat, et al., 2024, Todd et al., 2019a, Todd et al., 2019a). Although the exact mechanism behind *agr* activation remains unidentified, it results in the production of the effector molecule α-toxin, which can cause membrane damage, lysis, eicosanoid stimulation, disruption of tight junctions, activation of platelet aggregation, and dysregulation of the hemostatic system, ultimately leading to organ failure (Todd and Peters, 2019c).

Further studies elucidating the details of the "lethal synergism" among this interkingdom association will aid in the development of new therapeutic targets. The understanding of microbial interactions makes it clearer that the successful treatment of polymicrobial infections will arise from targeting the community as a whole (Lin, et al., 2013). For this reason, the present study aimed to investigate colony changes resulting from non-physical but close interactions in a long-term *C. albicans* and *S. aureus* co-culture. To that end, proximity assays confronting the yeast and bacteria at six different distances for 9 days were developed. We found that *S. aureus* virulence enhancement results from progressive phenotypical diversification of the original colonies.

2. Materials and methods

2.1. Bacterial strains and growing conditions

The fungaemia clinical isolates *Candida albicans* 10045727 and *Candida parapsilosis* 11103595 (Marcos-Zambrano, et al., 2014), and the bacterial strains *Staphylococcus aureus* ATCC 12600 (CECT 86), *Staphylococcus epidermidis* ATCC 1798 (CECT 231), *Streptococcus mutans* ATCC 25175 (CECT 479), *Enterococcus faecalis* ATCC 19433 (CECT 481) and *Escherichia coli* CFT073 (ATCC 700928) were used in this study. Each microorganism was recovered from a -80 stock. Bacteria were cultured at 37 ºC in Tryptic Soy Agar (TSA) (Scharlab S.L.) or Luria Bertani (LB) agar (Scharlab S.L.), while fungi were grown at 30 ºC in Yeast Petone Dextrose (YPD) medium consisting of 1 % Yeast Extract (Gibco), 2 % Meat Peptone (Scharlab S.L.), 2 % D-glucose (Fisher Scientific S.L.), and, when required, 2 % Bacteriological Agar (Scharlab S.L.). Similarly, overnight cultures were obtained after 16 h of incubation at 200 rpm and 30 ºC in YPD for *Candida* and 37 ºC in Tryptic Soy Broth (TSB) (Scharlab S.L.) or LB broth for bacterial strains.

2.2. Proximity assays

Overnight cultures of *C. albicans* and *S. aureus* were centrifuged at 4000 rpm (Labnet Spectrafuge™ 6C) for 5 min and washed twice with Phosphate Buffer Saline 1X (PBS) (Fisher Scientific S.L.). Suspensions with a final optical density of $\lambda = 550$ nm (OD_{550}) of 0.1 for yeast and 0.005 for bacteria ($\sim 1 \times 10^6$ CFUs/mL of both microorganisms) were prepared in PBS. Then, a 5 µl drop of each suspension was deposited in two parallel columns on YPD agar in a manner where the distance between both microorganism drops increased progressively (Ca – Sa). To ensure homogeneity and reproducibility at drop disposition a template was placed under the Petri dishes. In total, six different distances were tested: P1 = 1 cm, P2 = 1.5 cm, P3 = 2 cm, P4 = 3 cm, P5 = 4 cm, and P6 = 5 cm. Petri dishes were incubated at 37 °C for 9 days, and colony growth were recorded by imaging with the colony counter ProtoCOL 3 (Synbiosis). All images were processed with ImageJ software. Controls were created by facing drops from the same microorganism (Sa – Sa and Ca – Ca). Experiments were conducted thrice with 3 technical replicates each time. The same procedure was followed using YPD agar with Bromocresol purple at 0.08 mg/ml, denoted as YPD + BP, and YPD agar prepared with low D-glucose content (0.2 %), referred as YPLD.

Finally, we used a slightly modified proximity assay to confirm the pH influence on *S. aureus* colonies. First, a 5 µl drop from an *S. aureus* suspension was deposited on the agar in each corresponding position, leaving the facing positions empty. From day 1 to day 3, a 10 µl drop of a solution of NaOH 2M was applied in the morning and afternoon to the facing positions. On day 4, the drop quantity was increased to 15 µl, and on day 6, to 20 µl. This periodic addition of NaOH 2M, combined with its progressive quantity increase, simulated the continuous alkalinization of the medium by a growing colony of *C. albicans*. *S. aureus* responses were monitored until day 7. Control plates followed the same procedure but with the addition of PBS.

To confirm the specificity of the observed interactions between *C. albicans* and *S. aureus*, additional proximity assays were conducted using both microorganisms against different species (*S. epidermidis, S. mutans, E. coli, E. faecalis* and *C. parapsilosis*). Required controls were also included.

2.3. Virulence assessment of S. aureus colony variants

Differences in the virulence of the obtained colonies of *S. aureus* growing in the different positions of the proximity assay with *C. albicans* were evaluated using the animal model *G. mellonella*. Maintenance and injection of *G. mellonella* larvae were carried out, as previously reported by our laboratory (Moya-Andérico, et al., 2021).

Six different colonies of *S. aureus* from the proximity assays with *C. albicans* (Ca – Sa) were obtained after 10 days of incubation (Fig. 5A). Control colonies were obtained from control plates of *S. aureus* – *S. aureus* (Sa – Sa) after 10 days and 1 day of incubation (Fig. 5A). Cells were recovered directly from the agar plate with a pipette tip, resuspended in PBS, adjusted until an $OD_{550} = 1.8$, and injected into the hemocoel of eight larvae using a 26-gauge microsyringe (Hamilton). PBS-treated larvae were included as controls. The experiment was conducted three times, and larvae were monitored for a total of 48 h post-injection with intervals of 2h from 15 h-25 h and 40-48 h.

At the same time, 100 µl of *S. aureus* cell suspensions were centrifugated (4000 rpm x 1 min) and resuspended in a solution 1:10 of the resazurin-based reagent PrestoBlue in TSB media. After 30 min at 37 °C in the dark, the metabolic activity of the colonies was measured by fluorescence (λExc = 535 nm and λem=635 nm) and OD_{570} in a SPARK Multimode microplate reader. The remaining volume of cell suspensions was mixed with 500 mL of the stabilization solution RNAlater (Invitrogen) and frozen at -20 °C until further processing.

2.4. Characterization of gene expression of S. aureus colony variants

Cells suspensions of *S. aureus* colonies 1-5 obtained in a proximity assay with *C. albicans* (Ca – Sa) were used for RNA extraction using the GeneJET RNA Purification Kit (Thermo Fisher Scientific). RNA obtained was treated with 10x TURBO DNase (Life technologies). DNA contamination was discarded by PCR amplification of the 16S rRNA housekeeping gene. RNA quantification was performed on a NanoDrop 1000 Spectrophotometer (Thermo Fisher Scientific). Reverse transcription of RNA was performed by mixing the Maxima Reverse Transcriptase (Thermo Fisher Scientific) with Random Hexamer primers (Thermo Fisher Scientific) according to the manufacturer's instructions. The obtained cDNA was stored at -20 °C until use.

Quantitative real-time PCR (qRT-PCR) was performed with the

PowerUp SYBR Green Master Mix (Applied Biosystems) in a StepOnePlus™ Real-Time PCR System (Applied Biosystems) according to the manufacturer's protocol. The sequences of primers used for gene amplification can be consulted at Vaudaux et al., 2002 (Vaudaux, et al., 2002). Relative expression of RNA III, *agrA* and *sarA* genes were calculated using the values from control colony 8.

2.5. Reversion test of S. aureus colony variants

A small inoculum of each colony of *S. aureus* were taken at the end of a proximity assay (Ca – Sa) with a pipette tip and plated on a new YPD plate. The same procedure was performed with control colonies (Sa – Sa). After 24 h of incubation, the growth of the colonies was evaluated.

2.6. Statistical analysis

All data were statistically analyzed using GraphPad Prism version 10.00 (GraphPad Software, USA). Comparison of means among groups was performed by One-way ANOVA tests with a Šídák's multiple comparisons test. Log-rank tests made the comparison of Kaplan-Meier survival curves. A p-value <0.05 was considered statistically significant.

3. Results

3.1. C. albicans proximity promotes the generation of S. aureus colony variants

We observed non-physical interactions between the well-known opportunistic pathogens *S. aureus* (Sa) and *C. albicans* (Ca) through a proximity assay spanning six different distances over 9 days (Fig. 1). Inoculum drops deposited on the agar allowed for the development of well-defined colonies of both microorganisms, which were visible from day 1. In the case of *C. albicans*, colonies expanded progressively over the days. However, in the control (Ca – Ca), the size of the colonies decreased with increasing proximity, while in the proximity assay (Ca – Sa), the size remained constant across positions (Fig. S1).

In contrast, the size of *S. aureus* colonies in the proximity assay (Ca – Sa) remained constant (Fig. 1). However, between days 5 and 7, minor points of additional growth of *S. aureus* were observed within the original colony (see Fig. 1 small white arrows). The quantity and size of the growth spots increased over time, leading to fusion and covering the original colony entirely. By days 7-9, the expansion of new *S. aureus* colonies continued and extended beyond the edges of the original colonies (see Fig. 1 small white arrows). Interestingly, the emergence of

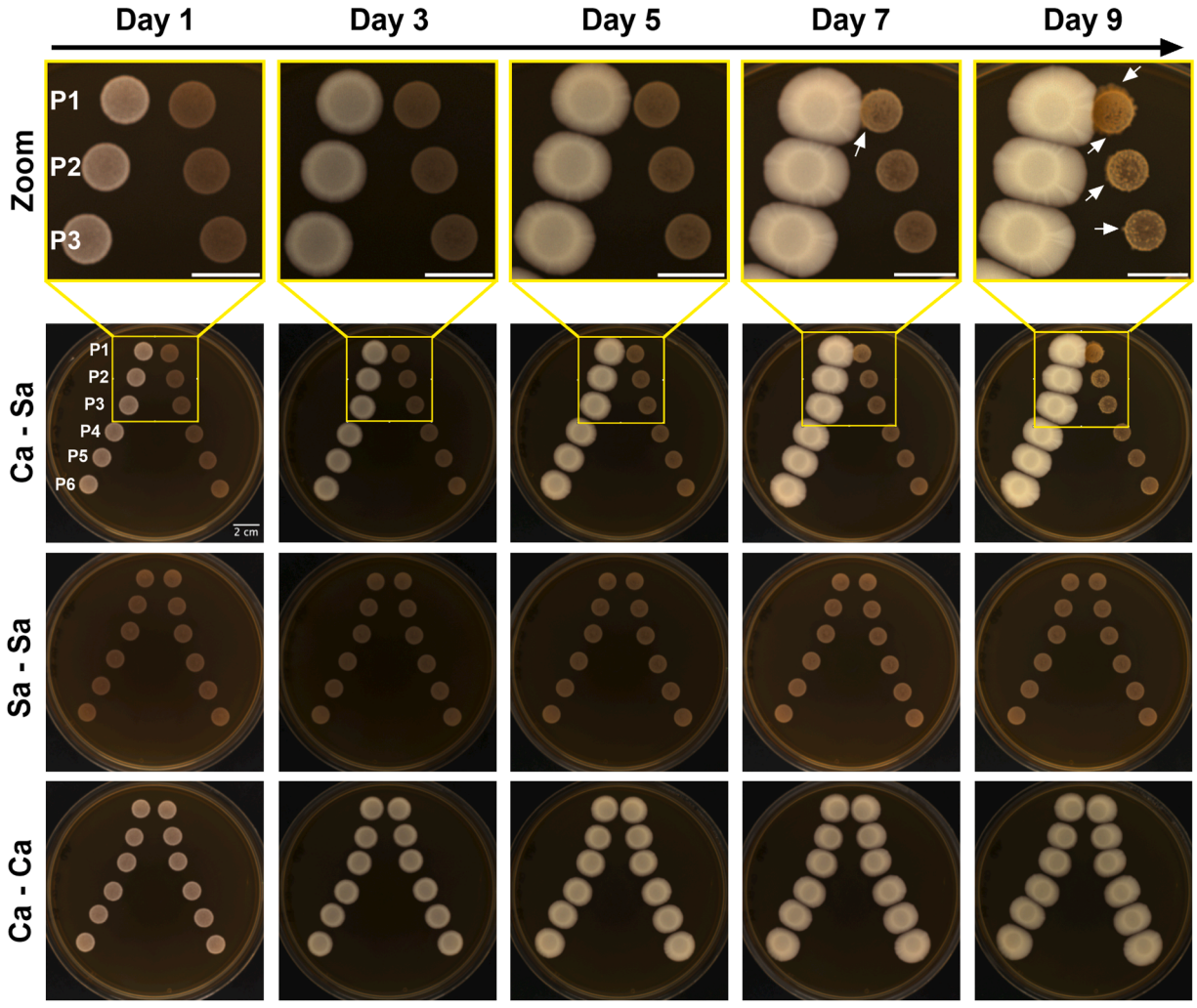

Fig. 1. Proximity assay timeline of *C. albicans* (Ca) and *S. aureus* (Sa). Ca – Sa depicts zoomed (top) and original images (bottom) of *C. albicans* colonies (left) developed at six different distances (P1 = 1 cm, P2 = 1.5 cm, P3 = 2 cm, P4 = 3 cm, P5 = 4 cm and P6 = 5 cm) from *S. aureus* colonies (right) monitored over 9 days with a 1-day interval. White arrows indicate evident growth of new phenotypes within *S. aureus* original colonies. Sa – Sa represents the control condition in which *S. aureus* inoculum was used in both columns, while Ca – Ca is the control condition where *C. albicans* inoculum was used in both columns. The images displayed are representative of three different experiments that were processed with ImageJ software. The scale bar of 2 cm applies to all cases.

new phenotypes was linked to the proximity to *C. albicans*, where the process of generating new variants was faster at the closest position (P1 = 1 cm). Consequently, the effect gradually decreased over subsequent positions, being minimal in the last ones (P5 = 4 cm and P6 = 5 cm) and absent in the control plate (Sa – Sa).

The described production of new *S. aureus* colonies was absent in proximity assays with other bacteria but were present with *Candida parapsilosis* (Fig. 2), indicating that the colony generation effect could be a specific interaction of *S. aureus* with the genus *Candida*.

3.2. Generation of S. aureus colony variants depend on pH and initial glucose levels

Considering the ability of *C. albicans* to alkalinize the media and the influence of pH on *S. aureus* virulence (Regassa and Betley, 1992, Regassa, et al., 1992, Todd et al., 2019a, Vylkova and Lorenz, 2014), we evaluated whether the appearance of *S. aureus* colony variants induced by *C. albicans* was related to pH changes. To this end, we performed the proximity assay by adding the pH indicator Bromocresol purple to the YPD agar medium (Fig. 3). The Sa – Sa control revealed that *S. aureus* growth from day 1 was accompanied by a pH decrease, which persisted throughout the experiment. In contrast, Ca – Ca control demonstrated that *C. albicans* growth led to a progressive increase in pH. These individual behaviors were maintained when both microorganisms were grown together (Ca – Sa). However, we observed that after day 5, *C. albicans* proximity to *S. aureus* nullified bacterial acidification. This alkalinization resulted in a predominance of a neutral pH in the positions with closer proximity between the species (P1-P3) by day 9. However, the most meaningful finding was the perfect overlap between *C. albicans* pH modulation and the origination of *S. aureus* colony variants (Fig. 3). Thus, we tested if *C. albicans* induced the formation of colony variants in other bacterial species, finding positive results with *S. epidermidis* and *E. coli* (Fig. S2).

Next, we assessed if the sole action of pH alkalinization was sufficient to induce the generation of *S. aureus* colony variants. Thus, we exposed *S. aureus* colonies grown in a proximity assay configuration to increasing quantities of NaOH 2M for 7 days (Fig. 4A). Again, we observed the appearance of *S. aureus* colony variants in positions (P1-P3) with greater exposure to pH changes. As expected, the PBS control did not induce either pH changes or the generation of *S. aureus* variant colonies. This finding showed that the presence of *C. albicans* is not necessary to obtain the phenotypic variants of *S. aureus* even though, in the case of proximity assays, it is responsible for this pH change.

Furthermore, we decided to test the role of glucose in the development of *S. aureus* colony variants, considering that glucose availability was reported to influence the Staphylococcal *agr* system (Regassa, et al., 1992) (Fig. 4B). A proximity assay between *S. aureus* and *C. albicans* in YPD with low glucose (YPLD) showed substantial variations in the growth of both microorganisms. Firstly, *C. albicans* growth decreased compared to YPD colonies, reflected in a smaller colony size at the end of the experiment in the control (Ca – Ca) and, more markedly, in the interaction with *S. aureus* (Ca – Sa). In contrast, *S. aureus* colonies growing in YPLD expanded over time, reaching a colony size considerably higher than when they grew in YPD, regardless of the presence of *C. albicans*. Additionally, *S. aureus* growth was not accompanied by the acidification of the media, resulting in the total dominance of *C. albicans* alkalinization and the pH neutralization of the complete plate. These changes did not promote the generation of *S. aureus* colony variants.

3.3. S. aureus colony variants exhibit increased virulence

To assess virulence differences of *S. aureus* colony variants, we conducted a proximity assay for 10 days. Each *S. aureus* colony was designated with a number, including controls (Fig. 5A). Colonies 1 to 4 corresponded to the phenotypes present at P1-P3 positions, where colony 4 represented the phenotype developed after initial exposure to

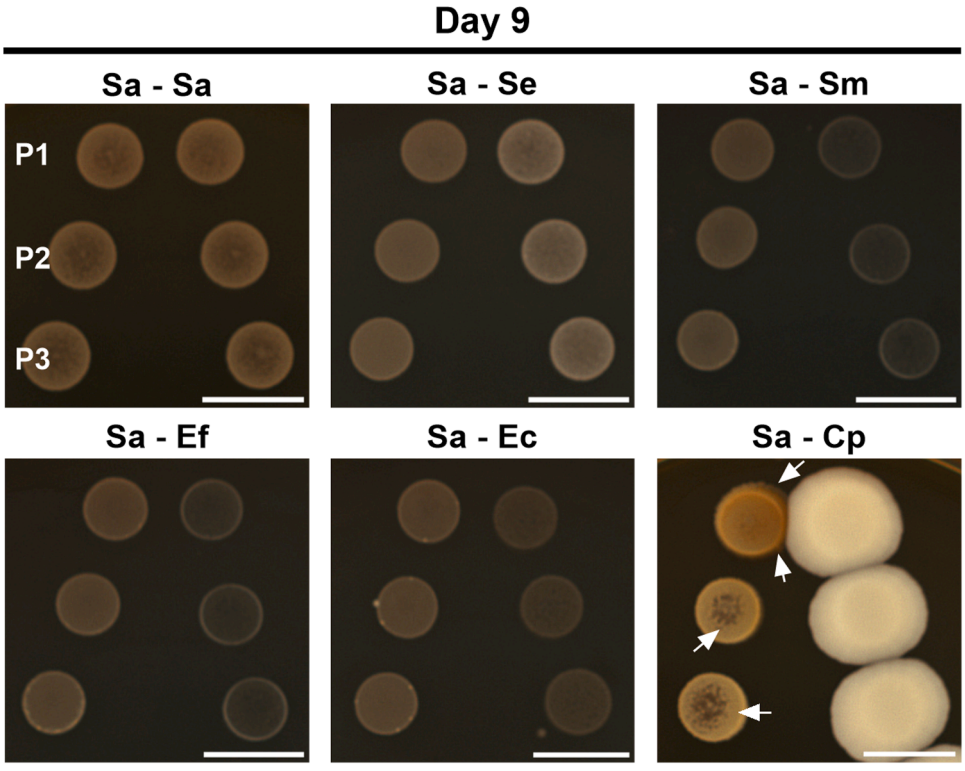

Fig. 2. Proximity assay of *S. aureus* (Sa) with other microorganisms. Zoomed images of *S. aureus* colonies (left) with itself (Sa – Sa), *S. epidermidis* (Sa – Se), *S. mutans* (Sa – Sm), *E. faecalis* (Sa – Ef), *E. coli* (Sa – Ec) and *C. parapsilosis* (Sa – Cp) (right) at day 9. The images displayed are representative of three different experiments that were processed with ImageJ software. The scale bar corresponds to 2 cm and applies to all cases. The shown distances correspond to P1 = 1 cm, P2 = 1.5 cm and P3 = 2 cm.

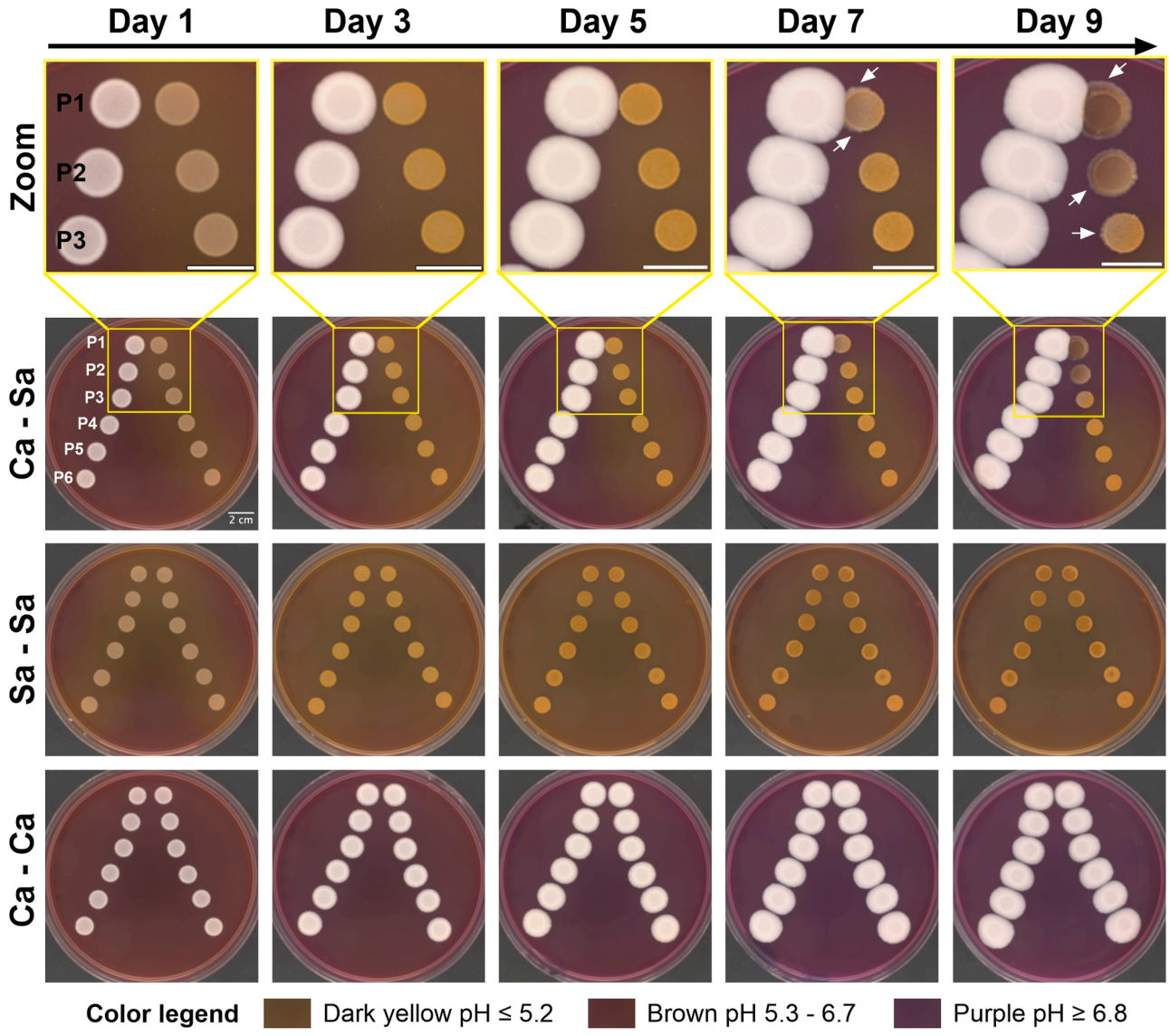

Fig. 3. Timeline of pH changes in a proximity assay of *C. albicans* (Ca) and *S. aureus* (Sa). Ca – Sa depicts zoomed (top) and original images (bottom) of *C. albicans* colonies (left) developed at six different distances from *S. aureus* colonies (right) in YPD agar with bromocresol purple. Plates were monitored over 9 days with a 1-day interval. White arrows indicate evident growth of new phenotypes within *S. aureus* original colonies. Sa – Sa represents the control condition in which *S. aureus* inoculum was used in both columns, while Ca – Ca is the control condition where *C. albicans* inoculum was used in both columns. The images displayed are representative of three different experiments that were processed with ImageJ software. The scale bar of 2 cm applies to all cases. The shown distances correspond to P1 = 1 cm, P2 = 1.5 cm, P3 = 2 cm, P4 = 3 cm, P5 = 4 cm, and P6 = 5 cm.

basic pH, and colony 1 represented the phenotype obtained after sustained exposure. Colonies 5 and 6 corresponded to the border and center of *S. aureus* growth at positions P4-P6, where no meaningful pH change was present. Controls were taken from a Sa – Sa plate incubated for 10 days (colony 7) and 1 day (colony 8).

Infection of *G. mellonella* with *S. aureus* colonies showed significant differences in larval survival (Fig. 5B). Larvae infected with colonies 5, 6 and 7 did not show mortality. Meanwhile, the median survival of larvae infected with colonies 1, 2, 3, 4 and 8 was 15 h, 19 h, 21 h, 40 h and 40 h, respectively. According to the Log-rank test, colonies 1 and 2 exhibited enhanced virulence compared to control colony 8. These variations cannot be attributed to differences in metabolic activity, as no statistically significant deviation was observed in the PrestoBlue results between colonies 1-5 and the control colony 8 (Fig. 5C). However, the lack of metabolic activity of colonies 6 and 7 justified the complete survival of larva infected with them.

Thus, the expression of three important virulence genes of *S. aureus* was evaluated in colonies 1-5 compared to control colony 8 (Fig. 5D–F). We found that colony 1, the most virulent, exhibited increased expression of RNA III and *agrA* but decreased expression of *sarA*. This *agrA* induction and *sarA* expression reduction were more pronounced in colony 2, although no change in RNA III was observed in this case. Colonies 3-5 showed decreased expression of all genes; however, repression of the *agrA* gene was higher in colony 5 compared to colonies 3 and 4. Therefore, the increased virulence of *S. aureus* variant colonies 1-4, which originated in response to external pH changes, compared to the original colony 6 and the control colonies 7 y 8, is associated with expression changes of genes from the *agr* system.

Finally, the colonies' re-plating showed no differences in their growth and morphology (Fig. 5G), indicating that the colony variants' phenotype is reversible. Moreover, the lack of growth of colonies 6 and 7 indicates that these populations are dead at the end of the experiment (10 days of incubation), confirming the results obtained by the PrestoBlue assay (Fig. 5C).

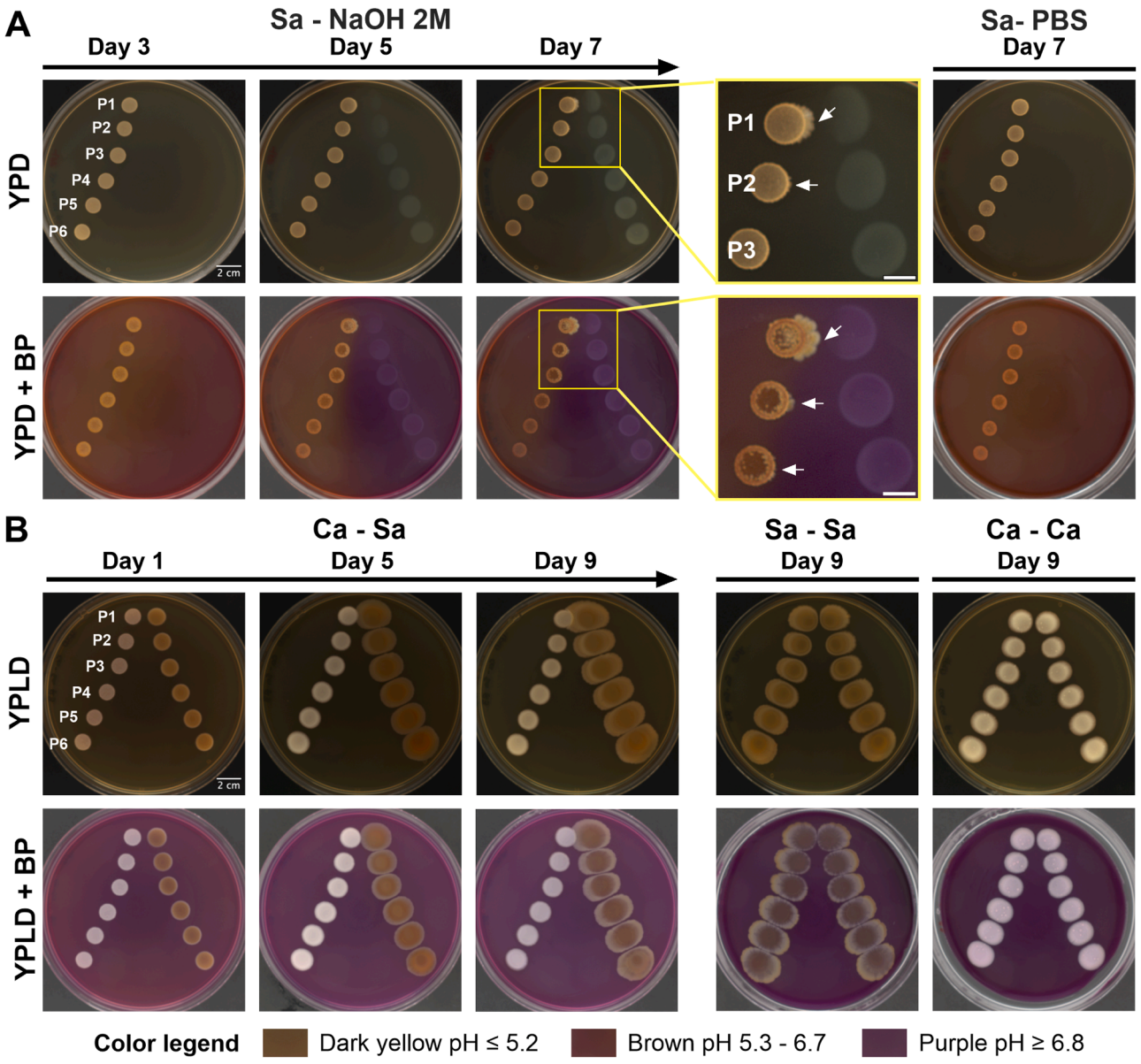

Fig. 4. pH and glucose dependence in the generation of *S. aureus* colony variants. Timeline of the effect of *S. aureus* colonies' exposure to NaOH 2M (Sa – NaOH 2M) in both YPD and YPD with bromocresol purple (YPD + BP) (A). Zoomed images from day 7 are displayed. White arrows indicate evident growth of new phenotypes within *S. aureus* original colonies. Sa – PBS represents the control condition. Timeline of glucose effect on *S. aureus* variant colonies' generation in a proximity assay of *S. aureus* with *C. albicans* (Ca – Sa) in both YPLD (YPD with glucose at 0.2 %) and YPLD with bromocresol purple (YPLD + BP) (B). Sa – Sa is the control condition in which *S. aureus* inoculum was used in both columns, while Ca – Ca is the control condition where *C. albicans* inoculum was used in both columns. The images displayed are representative of three different experiments that were processed with ImageJ software. The scale bar of 2 cm applies to all cases. The shown distances correspond to P1 = 1 cm, P2 = 1.5 cm, P3 = 2 cm, P4 = 3 cm, P5 = 4 cm, and P6 = 5 cm.

4. Discussion

The ability of both *C. albicans* and *S. aureus* to colonize a wide variety of human body sites increases the likelihood of shared host niches and the development of mixed infections (Eichelberger and Cassat, 2021). Survival in different microenvironments requires metabolic flexibility controlled by time- and space-specific regulatory networks (Jenul and Horswill, 2019, Richardson, 2019). This implies that environmental factors can influence disease outcomes (Todd et al., 2019a). Moreover, in the context of polymicrobial infections, the environmental response of one microorganism can affect the behavior of other species (Todd et al., 2019a).

In the case of *S. aureus*, the regulatory network controlling virulence responds to various environmental cues that drive the bacterium throughout the infection process (Jenul and Horswill, 2019). For instance, the *agr* system, responsible for RNA III expression and α-toxin secretion, is sensitive to acidic or alkaline conditions, with a maximum activity near neutral pH (Regassa and Betley, 1992, Regassa, et al., 1992, Todd and Peters, 2019c). Furthermore, *S. aureus* virulence is enhanced by *C. albicans,* resulting in what is described as lethal synergism (Carlson, 1982). Recent studies have shown that this effect is associated with increased *S. aureus* α-toxin production via *agr* activation in response to extracellular ribose depletion and media neutralization caused by *C. albicans* (Saikat, et al., 2024, Todd et al., 2019a, Todd et al., 2019a). However, questions regarding this cooperative microbial interaction mediated by environmental crosstalk remain.

In this study, we performed a proximity assay that allowed us to monitor colony changes resulting from non-physical interactions

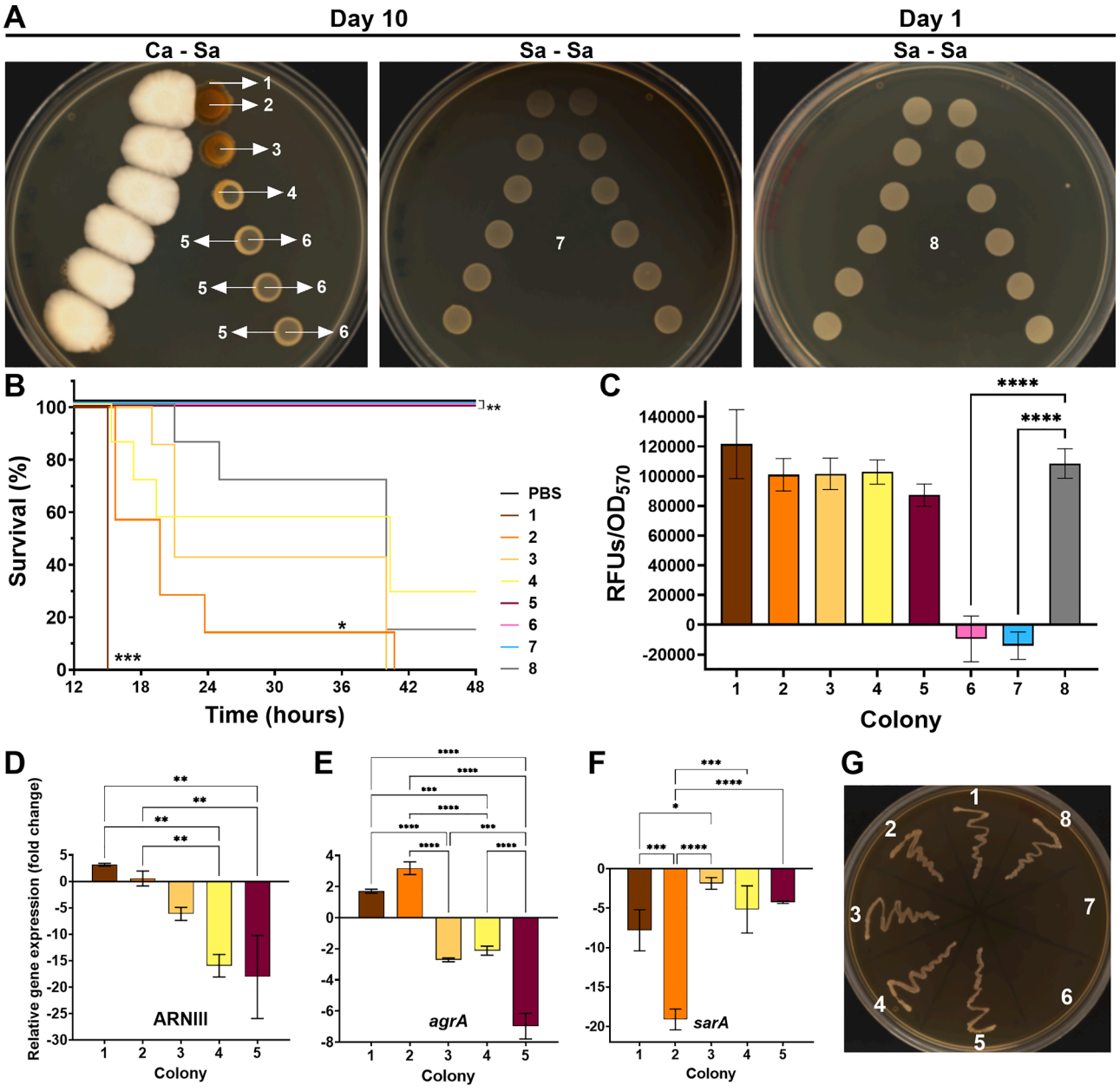

Fig. 5. Virulence assessment of *S. aureus* colony variants. Colonies of *S. aureus* obtained after a proximity assay with *C. albicans* (Ca – Sa) for 10 days were numbered (A). Colonies obtained from *S. aureus* controls (Sa – Sa) on day 10 and day 1 were also included. The shown distances correspond to P1 = 1 cm, P2 = 1.5 cm and P3 = 2 cm, P4 = 3 cm, P5 = 4 cm, and P6 = 5 cm. Kaplan-Meier survival curves of *G. mellonella* larvae after inoculation with all different *S. aureus* colonies, with each condition involving 8 larvae (B). Asterisks indicate statistically significant differences in virulence in comparison to control colony 8 by a long-rank test. Evaluation of the metabolic activity of *S. aureus* colonies by PrestoBlue assay (C). Asterisks indicate statistically significant differences versus control colony 8 in an Ordinary one-way ANOVA with Šidák's multiple comparison test. RFUs = Relative Fluorescence Units. Fold change of RNA III (D), *agrA* (E), and *sarA* (F) gene expression of *S. aureus* colonies 1-5 in comparison to control colony 8. Asterisks indicate statistically significant differences among colonies in an Ordinary one-way ANOVA with Šidák's multiple comparison test. Reversion test of *S. aureus* colonies (G). The results presented in this figure are representative of the same experiment repeated three times. Images were processed with ImageJ software, and error bars display mean and standard deviation. **p*-value <0.05, ***p*-value <0.01, ****p*-value <0.001, and *****p*-value <0.0001

between *S. aureus* and *C. albicans*. In contrast to previous studies that used liquid conditions for co-culture, our experiment permitted the simultaneous evaluation of six different distances between species growth. Long-term plate incubation (over 9-10 days) compensated for the higher diffusion times and loss of volatile compounds present in solid agar, allowing events to be recorded sequentially. As a result, our investigation reports that *C. albicans* enhances *S. aureus* virulence by inducing the generation of successive new colony variants (Figs. 1 and Fig. 5). The origin of the colony variants coincided with the pH change induced by *C. albicans*-mediated media alkalinization (Fig. 3). However, *C. albicans* is not strictly required for their generation, as their appearance under other artificial pH modulators (NaOH) was also confirmed (Fig. 4). Variant classification of *S. aureus* from the proximity assays (Ca – Sa), conducted to assess virulence differences (Fig. 5A), was based on visual morphological differences observed after extended incubation, compared to colony 7 on the control plate (Sa – Sa).

Notably, *G. mellonella* larvae survival (Fig. 5B) decreased in relation to the generation time of the colony variant. Colonies generated after prolonged exposure to *C. albicans* proximity (colonies 1-2) caused significantly higher mortality compared to those exposed for a shorter

time (colonies 3-4), barely exposed (colonies 5-6), or not exposed at all (colony 7-8) (Fig. 5A and B). This agrees with the lethal synergism observed from *in vivo* experiments of systemic and local infections after co-inoculating both microorganisms' (Carlson, 1982, Hu, et al., 2021, Sheehan, et al., 2020, Todd et al., 2019a, Vila, et al., 2021, Wu, et al., 2021). Our results showed that *G. mellonella* larvae survival at 24 h decreased from 71.4 % when infected with colony 8 to 0-14 % when infected with colonies 1 and 2, respectively. These values are consistent with the previous study by Sheehan *et al.* (2020) using this animal model, where larvae infected with *S. aureus* alone and combined with *C. albicans* showed a survival of 80 % vs 30 % at 24 h (Sheehan, et al., 2020).

Moreover, our experimental setting allowed us to recreate the interaction between both species and to evaluate the virulence of *S. aureus* colonies independently. The isolation of the different *S. aureus* colonies from the proximity assay before larvae inoculation (Fig. 5A) demonstrated that although *C. albicans* is responsible for the increase of *S. aureus* virulence, it is not required for the lethal effect. Additionally, the qRT-PCR results showed that the increase in *S. aureus* virulence is related to an up-regulation of RNA III and *agrA*, two important genes controlled by the *agr* system (Fig. 5D–E). Therefore, we believe the high pathogenicity of *S. aureus* colony variants originated after *C. albicans* exposure is related to an increase in α-toxin expression, as previously reported (Todd et al., 2019a), although we did not perform a direct detection of this molecule. In addition, the loss of the morphological differences after re-plating the colony variants (Fig. 5G) indicates a phenotype reversion after stimuli removal.

García-Betancur *et al.* (2017) described a genetic cell-fate program in *S. aureus* that leads to a phenotypic bifurcation in genetically identical cells during infection (García-Betancur, et al., 2017). Through a bimodal switch in the *agr* system, *S. aureus* forms two specialized subpopulations: one type produces toxins and induces acute bacteremia (*agr*-on cells), while the other supports biofilm formation, enabling chronic infections (*agr*-off cells). Extracellular signals can modulate the size of these subpopulations, thus influencing infection outcomes. For example, high Mg^{2+} levels in bone and kidney tissues favor the *agr*-off phenotype and encourage microbial aggregate formation (García-Betancur, et al., 2017).

We propose that the *S. aureus* colony variants observed in our study result from metabolic responses to environmental cues affecting virulence, in this case triggered by *C. albicans*. However, a limitation of our study is that we did not perform genomic or transcriptomic characterization of these variants. Future work should involve RNA-sequencing, genome-wide analysis, and gene expression profiling. Additionally, it is important to consider that colony variants that grew on top of the original colony (e.g. colonies 2 and 4) were recovered jointly and, therefore, represent a heterogeneous population.

Following our recent discoveries and those of others, we propose a hypothetical model of *C. albicans-S. aureus* metabolic interactions and microenvironmental changes that could result in the enhancement of *S. aureus* virulence through the generation of new variants (Fig. 6). First, the aerobic growth of *C. albicans* under high glucose couples the glycolysis pathway with the TCA cycle (Wijnants, et al., 2022). Although glucose is its preferred carbon source, this yeast can simultaneously metabolize alternative sources through enzymes from the gluconeogenic and glyoxylate cycle (Lorenz, 2013, Miramón and Lorenz, 2017, Sandai, et al., 2012, Williams and Lorenz, 2020). Meanwhile, *S. aureus* aerobic growth in glucose rich-media causes repression of the tricarboxylic acid (TCA) cycle by CcpA. Thus, pyruvate obtained from glycolysis is converted to acetate and excreted into the media, causing a pH decrease and downregulating the staphylococcal *agr* system (Regassa, et al., 1992, Richardson, 2019).

Acetate may serve as a source of acetyl-coA, the central intermediate in carbon metabolism (Bayot, et al., 2023). It is naturally present in blood and within macrophages and neutrophils (Bayot, et al., 2023). Once glucose is depleted, *C. albicans* can utilize acetate as a carbon source, enter the glyoxylate cycle, pass through the TCA cycle, and produce glucose in the gluconeogenic pathway (Wijnants, et al., 2022). Additionally, acetate at physiologically relevant concentrations up-regulates enzymes related to fatty acid metabolism (Bayot, et al., 2023). Therefore, this could explain the positive impact of *S. aureus* on *C. albicans* growth (as observed in Fig. S1).

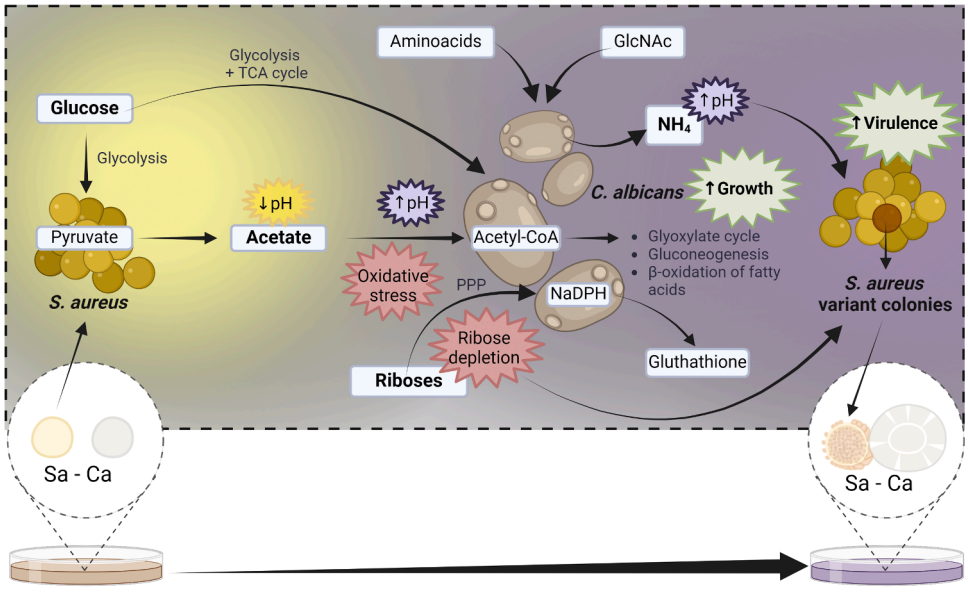

Fig. 6. Hypothetical proposed model of *S. aureus* and *C. albicans* metabolic interactions and their associated environmental changes influencing *S. aureus* virulence. *S. aureus* catabolism of glucose produces the excretion of acetate into the media, which decreases the pH. The acetate molecule serves as a precursor of acetyl-coA, positively impacting the growth of *C. albicans*. Acetate consumption through different metabolic routes helps neutralize the pH of the media in conjunction with ammonia (NH_4) production derived from amino acids and/or N-acetylglucosamine (GlcNAc) metabolism. Additionally, extracellular acetate can induce oxidative stress in *C. albicans* cells, leading to ribose metabolism in the Pentose Phosphate Pathway (PPP) to produce the required NADPH for glutathione synthesis. pH neutralization and ribose depletion of the media by *C. albicans* activate the Staphylococcal *agr* system, increasing *S. aureus* virulence. TCA = Tricarboxylic Acids. Image created with Biorender.com.

Furthermore, we believe that the consumption of acetate by *C. albicans* has an alkalinizing effect on the media, as reported with the metabolism of other carboxylic acids (α-ketoglutarate, pyruvate, and lactate) (Danhof Heather, et al., 2016). However, the environmental changes in pH exerted by *C. albicans* may also involve two alternative mechanisms that this yeast has evolved to counteract acidic environments (Danhof Heather, et al., 2016). The capacity to manipulate extracellular pH is related to survival inside phagocytic cells of the immune system and hyphal morphogenesis, being essential for fungal fitness *in vitro* and *in vivo* (Danhof Heather, et al., 2016, Vylkova and Lorenz, 2014). The metabolism of amino acids and N-acetylglucosamine results in ammonia externalization, leading to a pH increase in the media (Eichelberger and Cassat, 2021, Naseem, et al., 2017, Vesely, et al., 2017, Vylkova and Lorenz, 2014). This pH neutralization offers optimal conditions for the staphylococcal *agr* system, inducing α-toxin production (Eichelberger and Cassat, 2021).

Recently, the work of experts in the field, Peters and colleagues, discovered a fundamental role of *C. albicans* ribose catabolism in activating the *agr* system of *S. aureus* (Saikat, et al., 2024). Although our experiments do not evaluate this new factor, as were performed before the publication of this finding, we propose that *C. albicans* ribose catabolism may be related to the production of NADPH by the Pentose Phosphate Pathway (PPP) as a response to counteract the oxidative damage induced by acetate. Physiological relevant acetate concentrations have been shown to cause oxidative stress in *C. albicans* cells, leading to glutathione secretion into the media, and NADPH is an important molecule in the glutathione redox cycle (Bayot, et al., 2023, Komalapriya, et al., 2015, Wang, et al., 2006). Bringing all these points together suggests that the lethal synergism observed in *C. albicans* and *S. aureus* coinfection results from a series of metabolic interactions, including environmental changes to which both species react. Experiments focused on *C. albicans* acetate metabolism in this interkingdom co-culture will validate our hypothesis. Future studies should also consider including microenvironments more representative of infection sites, as it is unclear how these interactions influence *in vivo* outcomes.

The lack of growth of the original colonies 6 (Ca – Sa) and 7 (Sa – Sa) after replating (Fig. 5G) indicates that after 10 days of incubation on YPD agar plates, *S. aureus* bacteria cells are no longer viable. This was also shown by the PrestoBlue assay (Fig. 5C). Therefore, the presence of *C. albicans* favours and/or stimulates *S. aureus* survival by generating the colony variants, even in the furthest positions (P4-P6) where variant colony 5 appeared (Fig. 5A). This is not surprising, as *C. albicans* has been shown to stimulate *S. aureus* growth via PEG_2 secretion in both *in vitro* polymicrobial biofilms and *in vivo* polymicrobial infections (Krause, et al., 2015, Todd et al., 2019a).

Over time, the presence and proximity of *C. albicans* induce changes in *S. aureus* gene expression that increase its virulence, as seen in colonies 1-4 (Fig. 5). Although the underlying mechanism remains incompletely understood, there is growing evidence linking *S. aureus* metabolism with virulence, with an increasing number of metabolic transcriptional regulators influencing the expression of virulence factors (Richardson, 2019). For instance, ribose availability can alter the metabolic state of bacterial cells (Fig. 7), specifically affecting intracellular levels of ATP, GTP, and other metabolic intermediates (Hallier, et al., 2024, Nolan, et al., 2022). Ribose may thereby impact the expression of metabolic regulators such as CodY, a known repressor of the *agr* operon under nutrient-rich conditions (Roux, et al., 2014). Additionally, ribose might influence SigB activity via the RsbU-RsbV-RsbW cascade (Palma and Cheung, 2001). The transcriptional repressor RbsR, which regulates the operon involved in ribose uptake and phosphorylation (*rbsUDK*), is itself directly controlled by SigB, suggesting a potential feedback loop where SigB can impact ribose metabolism and vice versa (Lei and Lee, 2015).

Interspecific interactions between yeasts and *Staphylococcus* species have been reported to promote genotypic and phenotypic diversification of the bacteria (Cosetta, et al., 2023), opening the door to experiments with different strains of *S. aureus* and species of yeast. We highlight the utility of the proximity assay as a simple, inexpensive, and easy-to-implement technique for studying visible colony changes resulting from non-physical interactions among microorganisms. Its use

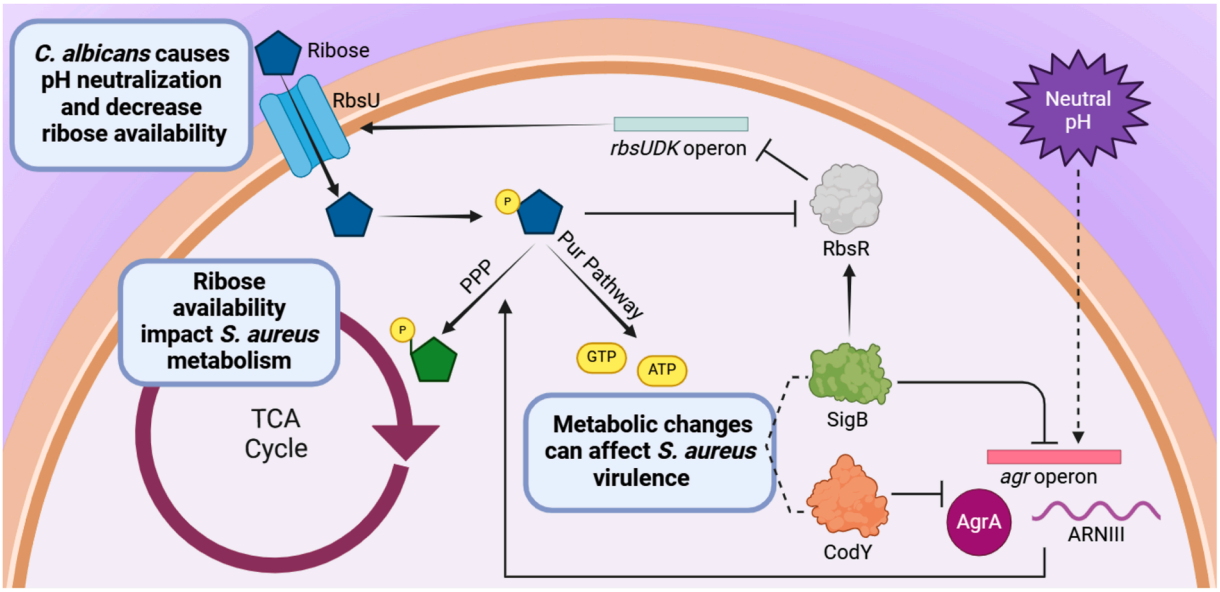

Fig. 7. Hypothetical interconnection between *S. aureus* metabolism and virulence in response to environmental modifications caused by *C. albicans*. *C. albicans* metabolism leads to pH neutralization and ribose depletion in the medium. Although the precise mechanisms by which these stimuli enhance *agr* system activity remain unclear, ribose is essential in key metabolic processes. It participates in both the Pentose Phosphate Pathway (PPP) and the Purine (Pur) pathway, influencing intracellular levels of ATP, GTP, Fructose-6-Phosphate, and other metabolites. Reduced ribose levels may affect metabolic regulators, such as CodY, a repressor of the *agr* operon under nutrient-rich conditions, and SigB, which plays a role in biofilm-related gene expression. Additionally, SigB activates the transcriptional repressor RbsR, which regulates the *rbsUDK* operon involved in ribose transport and phosphorylation. RNAIII may also impact ribose availability by activating PPP enzymes. This highlights the complex interplay between metabolism and virulence, where feedback loops are critical in regulating cellular function. TCA = Tricarboxylic Acids. Dashed lines represent unknown interactions. Image created with Biorender.com.

as a screening technique allowed us to identify similar interactions between *C. albicans* and two other bacterial pathogens, *S. epidermidis* and *E. coli*. Additionally, we found that the *C. parapsilosis* clinical isolate used in this study can alkalinize the pH (data not shown) and, therefore, induce the generation of *S. aureus* colony variants.

Our findings confirm that lethal synergistic effects between these microorganisms are associated with the *agr* system. Consequently, therapies targeting *agr* function could serve as effective alternatives against acute polymicrobial infections. In this context, researchers have identified several promising compounds: some inhibit AgrA binding to DNA (Bernabè, et al., 2021, Bezar, et al., 2019, Luo, et al., 2021), others interfere with quorum sensing (Sully, et al., 2014) or neutralize α-toxin (Todd et al., 2019a). Furthermore, considering the advantages *S. aureus* gains from the presence of *C. albicans,* antifungal treatments may help reduce bacterial burden in co-infections (Luo, et al., 2021). On the other hand, activation of the *agr* system by *C. albicans* may suggest that polymicrobial biofilms formed by these species have increased dispersal events. In this context, *C. albicans* may not only protect *S. aureus* cells but also enhance their dissemination, thereby increasing the risk of systemic infections.

5. Conclusion

For decades, it has been known that *C. albicans* increase *S. aureus* virulence, resulting in "lethal synergism". However, it is only recently that this phenomenon has begun to be characterized. Our experimental design allowed us to observe individual changes over time caused by the proximity of both microorganisms. As a result, we report for the first time that *C. albicans* proximity induces the generation and favors the growth of *S. aureus* colony variants with increased expression of virulence factors. The origin of these colony variants coincided with the pH change induced by *C. albicans*-mediated media alkalinization. The virulence factors are associated with the *agr* system, suggesting a role for α-toxin expression. These findings indicate that *S. aureus* enhanced lethality in *C. albicans* co-infections results from a series of metabolic interactions, highlighting the importance of understanding the intricate connection between environmental responses, virulence, and fitness in *S. aureus* pathogenesis.

Declaration of generative AI and AI-assisted technologies in the writing process

During the preparation of this work the authors used GPT-4 (openAI) to improve the readability and language of the manuscript. After using this tool/service, the authors reviewed and edited the content as needed and take full responsibility for the content of the published article.

CRediT authorship contribution statement

Betsy Verónica Arévalo-Jaimes: Conceptualization, Methodology, Investigation, Data curation, Formal analysis, Project administration, Writing – original draft. **Eduard Torrents:** Conceptualization, Project administration, Supervision, Methodology, Writing – review & editing.

Declaration of competing interest

The authors declare that they have no known competing financial interests or personal relationships that could have appeared to influence the work reported in this paper.

Acknowledgements

We thank Dr Jesus Guinea Ortega from the Department of Clinical Microbiology and Infectious Diseases, Hospital General Universitario Gregorio Marañón, Madrid, Spain, for the generous gift of the *Candida albicans* 10045727 and *Candida parapsilosis* 11103595 isolates used in this study.

Funding

This work was partially supported by grants PID2021-125801OB-100, PLEC2022-009356 and PDC2022-133577-I00 funded by MCIN/AEI/ 10.13039/501100011033 and "ERDF A way of making Europe", the CERCA programme and *AGAUR-Generalitat de Catalunya* (2021SGR01545), the European Regional Development Fund (FEDER) and Catalan Cystic Fibrosis association. The project that gave rise to these results received the support of a fellowship from the "la Caixa" Foundation (ID 100010434). The fellowship code is "LCF/BQ/DI20/11780040".

Funding sources were not involved in the research conduction or article preparation.

Supplementary materials

Supplementary material associated with this article can be found, in the online version, at doi:10.1016/j.crmicr.2024.100316.

Data availability

The datasets generated during and/or analysed during the current study are available from the corresponding author upon reasonable request.

References

Bayot, J., Martin, C., Chevreux, G., Camadro, J.-M., Auchère, F., 2023. The adaptive response to alternative carbon sources in the pathogen Candida albicans involves a remodeling of thiol- and glutathione-dependent redox status. Biochem. J. 480, 197–217. https://doi.org/10.1042/BCJ20220505.

Bernabè, G., Dal Pra, M., Ronca, V., Pauletto, A., Marzaro, G., Saluzzo, F., Stefani, A., Artusi, I., De Filippis, V., Ferlin, M.G., Brun, P., Castagliuolo, I., 2021. A novel aza-derivative inhibits agr quorum sensing signaling and synergizes methicillin-resistant Staphylococcus aureus to clindamycin. Front. Microbiol. 12. https://doi.org/10.3389/fmicb.2021.610859.

Bezar, I.F., Mashruwala, A.A., Boyd, J.M., Stock, A.M., 2019. Drug-like fragments inhibit agr-mediated virulence expression in Staphylococcus aureus. Sci. Rep. 9, 6786. https://doir.org/10.1038/s41598-019-42853-z.

Carlson, E., 1982. Synergistic effect of Candida albicans and Staphylococcus aureus on mouse mortality. Infect. Immun. 38, 921–924. https://doi.org/10.1128/iai.38.3.921-924.1982.

Carolus, H., Van Dyck, K., Van Dijck, P., 2019. Candida albicans and staphylococcus species: a threatening twosome. Front. Microbiol. 10, 2162. https://doi.org/10.3389/fmicb.2019.02162.

Cosetta, C.M., Niccum, B., Kamkari, N., Dente, M., Podniesinski, M., Wolfe, B.E., 2023. Bacterial–fungal interactions promote parallel evolution of global transcriptional regulators in a widespread Staphylococcus species. ISME J 17, 1504–1516. https://doi.org/10.1038/s41396-023-01462-5.

Danhof Heather, A., Vylkova, S., Vesely Elisa, M., Ford Amy, E., Gonzalez-Garay, M., Lorenz Michael, C., 2016. Robust extracellular pH modulation by Candida albicans during growth in carboxylic acids. mBio 7. https://doi.org/10.1128/mbio.01646-16.

Eichelberger, K.R., Cassat, J.E., 2021. Metabolic adaptations during Staphylococcus aureus and Candida albicans co-infection. Front. Immunol. 12. https://doi.org/10.3389/fimmu.2021.797550.

García-Betancur, J.-C., Goñi-Moreno, A., Horger, T., Schott, M., Sharan, M., Eikmeier, J., Wohlmuth, B., Zernecke, A., Ohlsen, K., Kuttler, C., Lopez, D., 2017. Cell differentiation defines acute and chronic infection cell types in Staphylococcus aureus. eLife 6, e28023. https://doir.org/10.7554/eLife.28023.

Hallier, M., Bronsard, J., Dréano, S., Sassi, M., Cattoir, V., Felden, B., Augagneur, Y., 2024. RANIII is linked with the pentose phosphate pathway through the activation of RpiRc in Staphylococcus aureus. mSphere 9 e00348-00323. https://doir.org/10.1128/msphere.00348-23.

Hu, Y., Niu, Y., Ye, X., Zhu, C., Tong, T., Zhou, Y., Zhou, X., Cheng, L., Ren, B., 2021. Staphylococcus aureus synergized with Candida albicans to increase the pathogenesis and drug resistance in cutaneous abscess and peritonitis murine models. Pathogens 10. https://doi.org/10.3390/pathogens10081036.

Jenul, C., Horswill, A.R., 2019. Regulation of Staphylococcus aureus virulence. Microbiol. Spectr. 7. https://doi.org/10.1128/microbiolspec.gpp3-0031-2018.

Kean, R., Rajendran, R., Haggarty, J., Townsend, E.M., Short, B., Burgess, K.E., Lang, S., Millington, O., Mackay, W.G., Williams, C., Ramage, G., 2017. Candida albicans mycofilms support Staphylococcus aureus colonization and enhances miconazole resistance in dual-species interactions. Front. Microbiol. 8. https://doi.org/10.3389/fmicb.2017.00258.

Komalapriya, C., Kaloriti, D., Tillmann, A.T., Yin, Z., Herrero-de-Dios, C., Jacobsen, M. D., Belmonte, R.C., Cameron, G., Haynes, K., Grebogi, C., de Moura, A.P.S., Gow, N. A.R., Thiel, M., Quinn, J., Brown, A.J.P., Romano, M.C., 2015. Integrative model of oxidative stress adaptation in the fungal pathogen Candida albicans. PLoS One 10, e0137750. https://doi.org/10.1371/journal.pone.0137750.

Kong, E.F., Tsui, C., Kucharíková, S., Andes, D., Van Dijck, P., Jabra-Rizk, M.A., 2016. Commensal protection of Staphylococcus aureus against antimicrobials by Candida albicans biofilm matrix. mBio 7. https://doi.org/10.1128/mbio.01365-16.

Krause, J., Geginat, G., Tammer, I., 2015. Prostaglandin E2 from Candida albicans stimulates the growth of Staphylococcus aureus in mixed biofilms. PLoS One 10 e0135404. https://doir.org/10.1371/journal.pone.0135404.

Lei, M.G., Lee, C.Y., 2015. RbsR activates capsule but represses the rbsUDK operon in Staphylococcus aureus. J Bacteriol 197, 3666–3675. https://doi.org/10.1128/JB.00640-15.

Lin, Y.J., Alsad, L., Vogel, F., Koppar, S., Nevarez, L., Auguste, F., Seymour, J., Syed, A., Christoph, K., Loomis, J.S., 2013. Interactions between Candida albicans and Staphylococcus aureus within mixed species biofilms. BIOS 84, 30–39. https://doi.org/10.1893/0005-3155-84.1.30.

Lorenz, M.C., 2013. Carbon catabolite control in Candida albicans: New wrinkles in metabolism. mBio 4. https://doi.org/10.1128/mbio.00034-13.

Luo, Y., McAuley, D.F., Fulton, C.R., J, S.P., McMullan, R., Lundy, F.T., 2021. Targeting Candida albicans in dual-species biofilms with antifungal treatment reduces Staphylococcus aureus and MRSA in vitro. PLoS One 16, e0249547. https://doir.org/10.1371/journal.pone.0249547.

Marcos-Zambrano, L.J., Escribano, P., Bouza, E., Guinea, J., 2014. Production of biofilm by Candida and non-Candida spp. Isolates causing fungemia: Comparison of biomass production and metabolic activity and development of cut-off points. Int. J. Med. Microbiol. 304, 1192–1198. https://doi.org/10.1016/j.ijmm.2014.08.012.

Miramón, P., Lorenz, M.C., 2017. A feast for Candida: Metabolic plasticity confers an edge for virulence. PLoS Pathog. 13, e1006144. https://doi.org/10.1371/journal.ppat.1006144.

Moya-Andérico, L., Admella, J., Torrents, E., 2021. A clearing protocol for Galleria mellonella larvae: Visualization of internalized fluorescent nanoparticles. N. Biotechnol. 60, 20–26. https://doi.org/10.1016/j.nbt.2020.08.002.

Naseem, S., Min, K., Spitzer, D., Gardin, J., Konopka, J.B., 2017. Regulation of hyphal growth and n-acetylglucosamine catabolism by two transcription factors in Candida albicans. Genet 206, 299. https://doi.org/10.1534/genetics.117.201491.

Nolan, A.C., Zeden Merve, S., Kviatkovski, I., Campbell, C., Urwin, L., Corrigan Rebecca, M., Gründling, A., O'Gara James, P., 2022. Purine nucleosides interfere with c-di-AMP levels and act as adjuvants to re-sensitize mrsa to β-lactam antibiotics. mBio 14 e02478-02422. https://doir.org/10.1128/mbio.02478-22.

Palma, M., Cheung, A.L., 2001. σb activity in staphylococcus aureus is controlled by rsbU and an additional factor(s) during bacterial growth. Infect. Immun. 69, 7858–7865. https://doir.org/10.1128/iai.69.12.7858-7865.2001.

Peters, B.M., Jabra-Rizk, M.A., O'May, G.A., Costerton, J.W., Shirtliff, M.E., 2012. Polymicrobial interactions: Impact on pathogenesis and human disease. Clin. Microbiol. Rev. 25, 193–213. https://doi.org/10.1128/CMR.00013-11.

Regassa, L.B., Betley, M.J., 1992. Alkaline pH decreases expression of the accessory gene regulator (agr) in Staphylococcus aureus. J. Bacteriol. 174, 5095–5100. https://doi.org/10.1128/jb.174.15.5095-5100.1992.

Regassa, L.B., Novick, R.P., Betley, M.J., 1992. Glucose and nonmaintained pH decrease expression of the accessory gene regulator (agr) in Staphylococcus aureus. Infect. Immun. 60, 3381–3388. https://doi.org/10.1128/iai.60.8.3381-3388.1992.

Richardson, A.R., 2019. Virulence and metabolism. Microbiol. Spectr. 7. https://doi.org/10.1128/microbiolspec.gpp3-0011-2018.

Roux, A., Todd, D.A., Velázquez, J.V., Cech, N.B., Sonenshein, A.L., 2014. CodY-mediated regulation of the Staphylococcus aureus agr system integrates nutritional and population density signals. J. Bacteriol. 196, 1184–1196. https://doir.org/10.1128/jb.00128-13.

Saikat, P., Todd, O.A., Eichelberger, K.R., Tkaczyk, C., Sellman, B.R., Noverr, M.C., Cassat, J.E., Fidel Jr., P.L., Peters, B.M., 2024. A fungal metabolic regulator underlies infectious synergism during Candida albicans-Staphylococcus aureus intra-abdominal co-infection. Nat. Commun. 15, 5746. https://doi.org/10.1038/s41467-024-50058-w.

Sandai, D., Yin, Z., Selway, L., Stead, D., Walker, J., Leach Michelle, D., Bohovych, I., Ene Iuliana, V., Kastora, S., Budge, S., Munro Carol, A., Odds Frank, C., Gow Neil, A.R., Brown Alistair, J.P., 2012. The evolutionary rewiring of ubiquitination targets has reprogrammed the regulation of carbon assimilation in the pathogenic yeast Candida albicans. mBio 3. https://doi.org/10.1128/mbio.00495-12.

Sheehan, G., Tully, L., Kavanagh, K.A., 2020. Candida albicans increases the pathogenicity of Staphylococcus aureus during polymicrobial infection of Galleria mellonella larvae. Microbiology 166, 375–385. https://doi.org/10.1099/mic.0.000892.

Sully, E.K., Malachowa, N., Elmore, B.O., Alexander, S.M., Femling, J.K., Gray, B.M., DeLeo, F.R., Otto, M., Cheung, A.L., Edwards, B.S., Sklar, L.A., Horswill, A.R., Hall, P.R., Gresham, H.D., 2014. Selective chemical inhibition of agr quorum sensing in Staphylococcus aureus promotes host defense with minimal impact on resistance. PLoS Pathog. 10, e1004174. https://doir.org/10.1371/journal.ppat.1004174.

Todd, O.A., Fidel Jr., P.L., Harro, J.M., Hilliard, J.J., Tkaczyk, C., Sellman, B.R., Noverr, M.C., Peters, B.M., 2019a. Candida albicans augments Staphylococcus aureus virulence by engaging the staphylococcal agr quorum sensing system. mBio 10. https://doi.org/10.1128/mbio.00910-19.

Todd, O.A., Peters, B.M., 2019b. Candida albicans and Staphylococcus aureus pathogenicity and polymicrobial interactions: Lessons beyond koch's postulates. J. Fungi. 5, 81. https://doi.org/10.3390/jof5030081.

Vaudaux, P., Francois, P., Bisognano, C., Kelley William, L., Lew Daniel, P., Schrenzel, J., Proctor Richard, A., McNamara Peter, J., Peters, G., Von Eiff, C., 2002. Increased expression of clumping factor and fibronectin-binding proteins by HemB mutants of Staphylococcus aureus expressing small colony variant phenotypes. Infect. Immun. 70, 5428–5437. https://doi.org/10.1128/iai.70.10.5428-5437.2002.

Vesely, E.M., Williams, R.B., Konopka, J.B., Lorenz, M.C., 2017. N-acetylglucosamine metabolism promotes survival of Candida albicans in the phagosome. mSphere 2. https://doi.org/10.1128/msphere.00357-17.

Vila, T., Kong, E.F., Montelongo-Jauregui, D., Van Dijck, P., Shetty, A.C., McCracken, C., Bruno, V.M., Jabra-Rizk, M.A., 2021. Therapeutic implications of C. albicans-S. aureus mixed biofilm in a murine subcutaneous catheter model of polymicrobial infection. Virulence 12, 835–851. https://doi.org/10.1080/21505594.2021.1894834.

Vylkova, S., Lorenz, M.C., 2014. Modulation of phagosomal ph by Candida albicans promotes hyphal morphogenesis and requires stp2p, a regulator of amino acid transport. PLoS Pathog. 10. https://doi.org/10.1371/journal.ppat.1003995 e1003995.

Wang, Y., Cao, Y.-Y., Jia, X.-M., Cao, Y.-B., Gao, P.-H., Fu, X.-P., Ying, K., Chen, W.-S., Jiang, Y.-Y., 2006. Cap1p is involved in multiple pathways of oxidative stress response in Candida albicans. Free Radic. Biol. Med. 40, 1201–1209. https://doi.org/10.1016/j.freeradbiomed.2005.11.019.

Wijnants, S., Vreys, J., Van Dijck, P., 2022. Interesting antifungal drug targets in the central metabolism of Candida albicans. Trends Pharmacol. Sci. 43, 69–79. https://doi.org/10.1016/j.tips.2021.10.003.

Williams, R.B., Lorenz, M.C., 2020. Multiple alternative carbon pathways combine to promote Candida albicans stress resistance, immune interactions, and virulence. mBio 11. https://doi.org/10.1128/mbio.03070-19.

Wu, Y.-M., Huang, P.-Y., Cheng, Y.-C., Lee, C.-H., Hsu, M.-C., Lu, J.-J., Wang, S.-H., 2021. Enhanced virulence of Candida albicans by Staphylococcus aureus: Evidence in clinical bloodstream infections and infected zebrafish embryos. J. Fungi. 7. https://doi.org/10.3390/jof7121099.